FEM SUBSYSTEM REPLACEMENT TECHNIQUES FOR STRENGTH PROBLEMS IN VARIABLE GEOMETRY TRUSSES.

Luis M. Macareno*, Josu Agirrebeitia, Carlos Angulo, Rafael Avilés

Department of Mechanical Engineering, University of the Basque Country

Alameda Urquijo s/n, 48013 Bilbao, Spain

* Corresponding author:

Luis M. Macareno

Department of Mechanical Engineering, University of the Basque Country UPV/EHU
Escuela Técnica Superior de Ingeniería, ETSI
Alameda de Urquijo s/n,
48013 Bilbao
SPAIN
Tel: +34 946017399, Fax: +34 946014215
E-mail: imbmaral@ehu.es

Number of words: 5267
Number of figures: 15
Tables: 2

Abstract

This work presents the application of a procedure for replacing FEM subsystems with a high number of dofs (possibility of including mobile internal parts) using Equivalent Parametric Macroelements (EPMs) with a much reduced number of elements to

decrease significantly the analysis time with an acceptable error. This procedure is applied to the replacement of VGT mobile joints. The equivalence criterion proposed is based on elastic strain energies absorbed by both bodies. Said replacement involves resolution of a redundant non-linear equation system, iteratively focused via linearization and subsequent resolution via the Least Squares Method. The search for initial approximation is supported by Genetic Algorithm techniques.

Key words: Variable Geometry Truss (VGT), Finite Element, Equivalent Parametric Macroelement (EPM), Energy Method, Optimization.

1. Introduction.

Variable geometry structures are those capable of modifying their geometry to adapt to different loads and working conditions. This is possible because some of the elements comprising them can vary their length. These elements are called actuators. Another characteristic making them interesting is their high stiffness to weight ratio, which has contributed to the application of variable geometry structures in the spatial research field. The study of these structures dates back to the 1980s [1]. A specific type within this group is based on spatial truss type structures known as Variable Geometry Truss (VGT). Its most common application is as manipulators [2, 3 and 4]. These trusses are formed via repetition of the main module whose topology can be highly varied [5, 6].The most widely known VGT is the Double Octahedral, made up of two main octahedral modules [7, 8, 9].

The MBAD[1] (Multi Body Analysis and Design) workgroup of the University of the Basque Country has developed a five-module VGT prototype, where the geometry of the main module is also established upon the octahedral shape. The real structure is shown in Fig. 1. Each module is a parallel kinematic mechanism in itself with actuators set on the horizontal planes. These planes are joined among them using fixed length bars called longerons. The joint between these bars and the actuators is done by special joints. These joints have also been developed by the workgroup and are patented. In Fig. 2 there is an exploded view of the joint where it can be appreciated the different elements comprising the same.

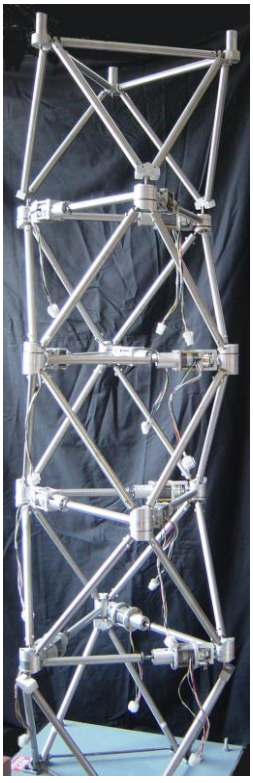

Fig. 1. Five-Module VGT Prototype

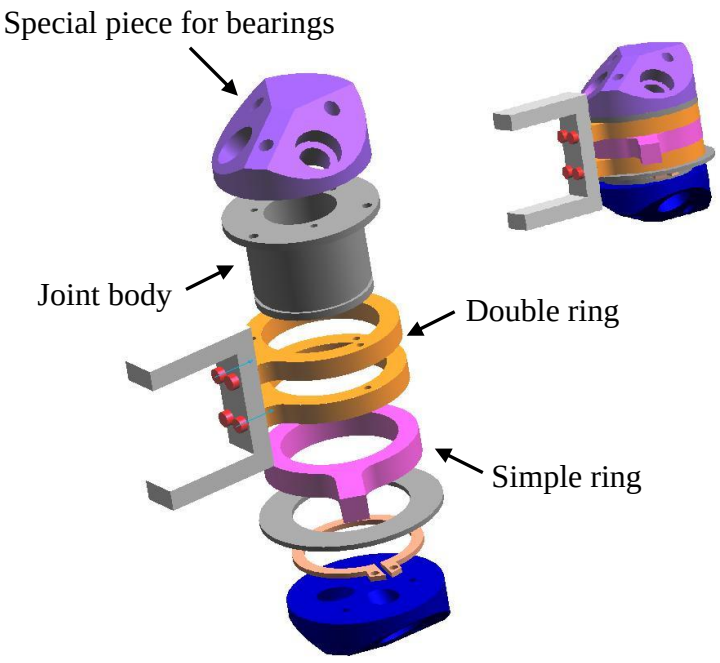

Fig. 2. Exploded view of the joint.

[1] *http://www.ehu.es/mbad*

To perform the analysis on the structure a finite element model was created in MSC/Nastran, preceded by another detailed cinematic model created using MSC/Adams. Fig. 3 shows both models indicating the different elements comprising the five-module VGT.

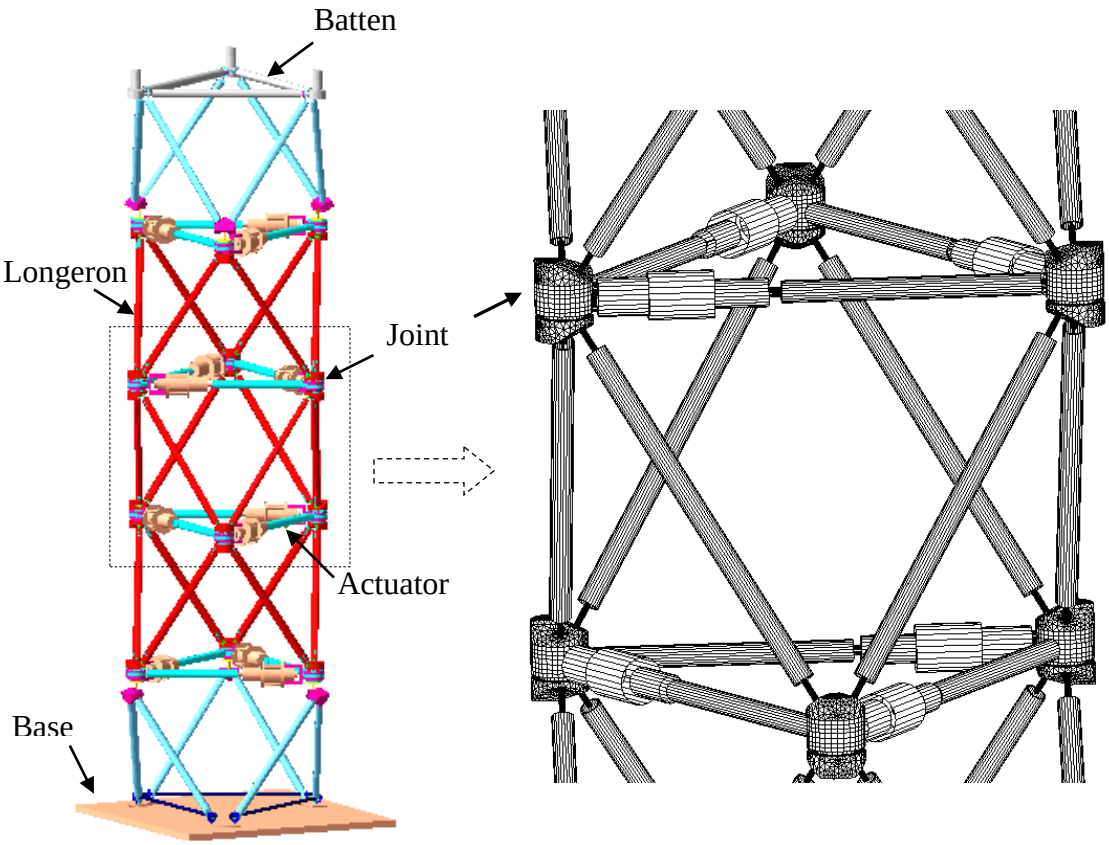

Fig. 3. VGT kinematic and FEM model

In these structures it is necessary to perform the analysis on various configurations. A program has been developed in PCL (Patran Command Language) which automatically creates a FEM model in each position to enable diverse studies. Once the FEM model of the variable geometry structure has been created, its behavior is studied under different load cases and in different positions. As this is a detailed model, both creation and analysis time are excessive, so the need to reduce the model arises. There are different static model reduction techniques, where the most widely known are reduction via static

condensation [10, 11], iterative techniques [12, 13], macroelements [14, 15] and substructuring techniques [16].

This paper presents the application of a static reduction technique for FEM models via replacement of certain submodels by equivalent parametric macroelements (EPMs). These macroelements will have a much lower number of elements than the submodels they replace, and consequently computation cost is drastically reduced. The technique is based on elastic strain energy equivalence between the submodel and its corresponding macroelement. This criterion has led to good results in other applications [17, 18].

The model to be analyzed is the variable geometry structure shown in Fig. 1, and the submodels to be replaced are the intermediate joints of the structure. These submodels consist of 3D tetrahedral and hexahedral type elements, likewise rigid and contact elements. Altogether there are approximately 2000 elements per submodel. Fig. 4 shows the FEM model of one of the joints.

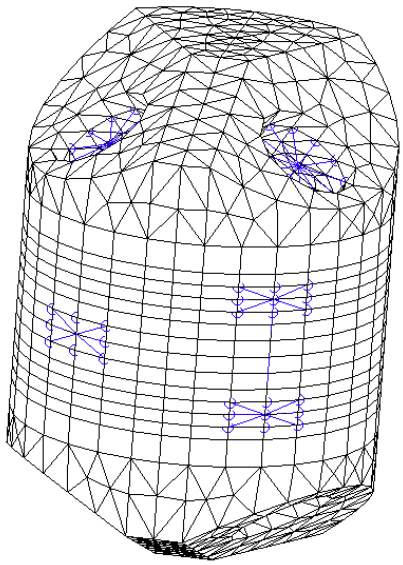

Fig. 4. Joint FEM Model

The following section defines the mathematical development of the macroelement in detail. Once its function has been understood, the methodology of the model reduction technique is explained; defining all the variables likewise the equations arising from energy equivalence. Below are the results obtained via application of this technique for the joint of the five-module VGT. Finally, a brief commentary on these results and the conclusions are shown.

2. Mathematical definition of the joint macroelement.

The macroelement as understood in this paper is a series of elements, which join together forming a new body. If this set of elements is intended to replace another model, it might satisfy certain restraints: firstly it must be cinematically equivalent to the replaced model and secondly equivalent from a structural viewpoint. The choice of the type of elements is free as far as the connections with the rest of the model and the internal mobility are preserved. In this case, the defined macroelement to replace the finite element submodel of the joint is formed by eight 3D beam elements with circular section and nine nodes, as shown in Fig. 5. Each of these nodes has six dofs, three translations (u_x, u_y, u_z) and three rotations (θ_x, θ_y, θ_z). The beams are arranged so nodes 1, 3, 6 and 7 correspond to the central points of the joint spherical bearings and nodes 8 and 9 to the link points of the rings with actuator bars. It can be appreciated node 9 really correspond to the point midway between the two link points of the double ring. Nodes 2, 4 and 5 are internal and have not physical correspondence with any of the joint. Node 4 is located on the central point belonging to the rotation axis of the joint rings. In Fig. 6 it can be appreciated the correspondence of the macroelement nodes with the joint submodel.

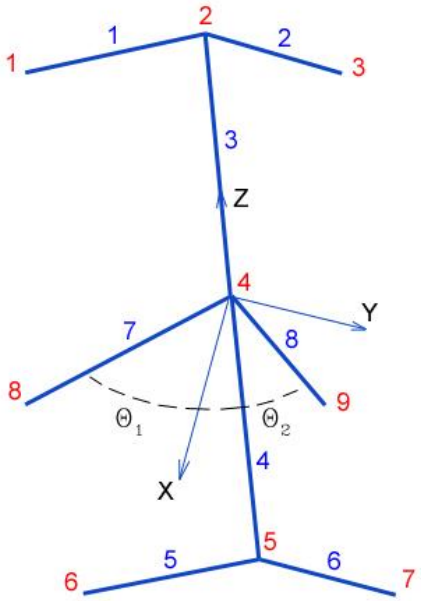

Fig. 5. Macroelement

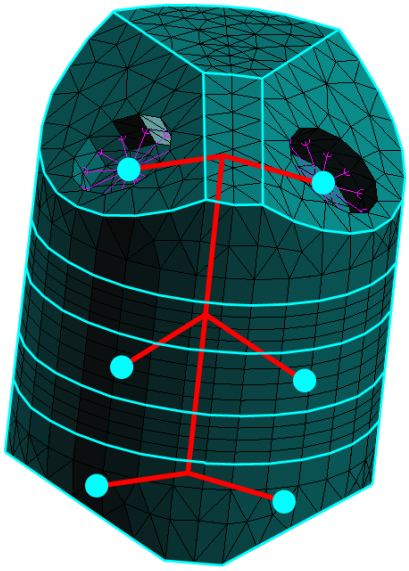

Fig. 6. Submodel and macroelement correspondence.

2.1 Stiffness matrix.

The macroelement stiffness matrix is obtained via the sum of expanded matrices of each element, once expressed into the global system. The axes of this global system are *XYZ* shown in Fig. 5. As the macroelement consists of 9 nodes each with 6 dofs, the final matrix is 54 x 54. The element matrices are 12 x 12, since 3D beam type elements were used.

As said before, the macroelement must be cinematically equivalent to the submodel. The rings round the joint body can rotate in relation to the central axis. These rotation

angles shown in Fig. 5 have been defined as θ_1 and θ_2. The rotation condition must be included in the macroelement. This has been done releasing the rotation dof regarding the central axis on the nodes corresponding to elements 7 and 8. These elements would correspond to the rings in the submodel. The fact of releasing dofs on a node is equal to including the null force transmission condition in the same direction. The node undergoing this situation is number 4, where four elements concur numbered 3, 4, 7 and 8. Elements 7 and 8, as mentioned before, would correspond to the rings and elements 3 and 4 would represent the central axis of the real joint. Therefore, contribution of the moment in direction *Z* on node 4 of elements 7 and 8 must be cancelled. Fig. 7 shows released dofs, likewise the local systems of elements 7 and 8. Anyway on this node, effort continues being transmitted in that direction, although only between elements 4 and 5. Introducing this condition means the stiffness matrix of elements 7 and 8 suffer certain modifications directly influencing the macroelement stiffness matrix. Below the mathematical development is shown in detail.

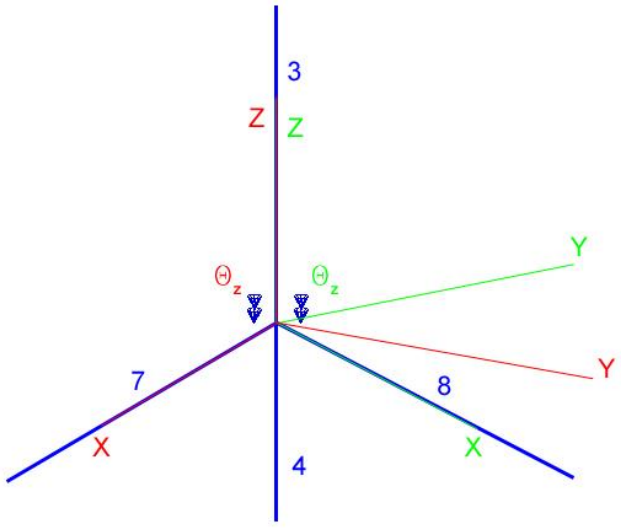

Fig. 7. Released dofs

Moment according to the released dof is not transmitted, so it is null. In element 7 it corresponds to M_z on the first node of the element. Thus, using its equilibrium equation (1) and equaling to zero it can be obtained the released dof which now becomes dependent on the rest.

$$M_{z1} = 0 = \frac{6 \cdot E \cdot I_z}{L^2} \cdot u_{y1} + \frac{4 \cdot E \cdot I_z}{L} \cdot \theta_{z1} - \frac{6 \cdot E \cdot I_z}{L^2} \cdot u_{y2} + \frac{2 \cdot E \cdot I_z}{L} \cdot \theta_{z2} \qquad (1)$$

$$\theta_{z1} = \frac{3}{2 \cdot L} \cdot (u_{y2} - u_{y1}) - \frac{\theta_{z2}}{2} \qquad (2)$$

Eq. (2) is replaced in all the matrix rows where term θ_{z1} appears and the new matrix is obtained. This matrix has zeros in all the row and column corresponding to the released dof. This development is analogous for element 8. All relevant matrices are shown on the Appendix.

Once the previous steps have been executed to achieve cinematic equivalence, the macroelement global stiffness matrix is obtained via coupling of all the matrices of each element in global coordinates.

At this point, the macroelement has been completely defined, which depends on the physical properties (E, υ, G) and dimensions of the elements comprising the same, such as the section or radii. Any of these variables may be selected as a parameter.

2.2 Macroelement stiffness matrix condensation.

The following step is to condense this matrix to a few numbers of dofs called masters. These master dofs must be chosen as they also exist in the submodel, in this case, the translation displacements in *x*, *y*, *z* of nodes 1, 3, 6, 7, 8 and 9. These nodes correspond with the ones which act as interface with the rest of the model.

The purpose is to obtain the macroelement strain energy just from the displacements of the master dofs. Complete execution of this condensation is detailed in [10], however, the basic ideas are shown below.

The formula used to calculate strain energy generically is:

$$V = \frac{1}{2} \cdot \{\delta\}^T \cdot [K] \cdot \{\delta\} \tag{3}$$

where $\{\delta\}$ is the displacement vector, which includes all the dofs. The aim of condensation is to reduce the number of dofs, where a new reduced matrix is obtained, which is still square and symmetric, although much denser than the original. The procedure requires the election of the master dofs, where the rest are slaves. A requirement of this technique is that no force acts on any slave dof. Eq. (4) relates the forces and displacements via the stiffness matrix.

$$[K] \cdot \{\delta\} = \{P\} \tag{4}$$

Eq. (4) can be rearranged bearing in mind the previously chosen master and slave dofs.

$$\begin{bmatrix} [k]_{mm} & [k]_{ms} \\ [k]_{sm} & [k]_{ss} \end{bmatrix} \cdot \begin{Bmatrix} \{\delta\}_m \\ \{\delta\}_s \end{Bmatrix} = \begin{Bmatrix} \{P\}_m \\ \{P\}_s \end{Bmatrix} \tag{5}$$

Developing the submatrix product and including the condition that the forces on the slave nodes are null, the following equations are obtained:

$$[k]_{mm} \cdot \{\delta\}_m + [k]_{ms} \cdot \{\delta\}_s = \{P\}_m \tag{6}$$

$$[k]_{sm} \cdot \{\delta\}_m + [k]_{ss} \cdot \{\delta\}_s = \{0\} \tag{7}$$

From Eq. (7), the vector of slave displacements is written as a function of the masters

$$\{\delta\}_s = -[k]_{ss}^{-1} \cdot [k]_{sm} \cdot \{\delta\}_m \tag{8}$$

and is replaced in Eq. (6), obtaining:

$$[k]_{mm} \cdot \{\delta\}_m - [k]_{ms} \cdot [k]_{ss}^{-1} \cdot [k]_{sm} \cdot \{\delta\}_m = \{P\}_m \tag{9}$$

Eq. (9) may be written:

$$[k]_{mm}^{r} \cdot \{\delta\}_m = \{P\}_m \tag{10}$$

being

$$[k]^r_{mm} = [k]_{mm} - [k]_{ms} \cdot [k]^{-1}_{ss} \cdot [k]_{sm} \tag{11}$$

This is the new stiffness matrix reduced to the master dofs and Eq. (12) is the new formula for obtaining the energy, which provides an identical value to that obtained via Eq. (3), where whole stiffness matrix and the displacements of all the dofs were used.

$$V^r = \frac{1}{2} \cdot \{\delta\}^T_m \cdot [k]^r_{mm} \cdot \{\delta\}_m \tag{12}$$

At this point, it has been explained the procedure to obtain the macroelement strain energy. Input variables are the displacements of the master dofs. However, the macroelement parameters must be defined and adjusted to achieve equivalence with the submodel. Here, the radii of the 3D beam elements with circular section have been chosen. Total number of parameters amounts to 8, likewise the number of elements. The stiffness matrix coefficients depend on these parameters and constants of the materials. It must not been forgotten that the two angles θ_1 and θ_2 also influence the matrix *[K]*, and likewise $[K]^r$. For the analyses performed in this study, the value of these angles has varied between 21 and 44 degrees. These are the maximum and minimum values when the structure is in its extreme positions.

3. Definition of the equivalence method.

The aim of the method is to find the values of some parameters which optimize the value of an equivalence function. As already mentioned, our study parameters are the radii of the macroelement beams. The function must be such as to indicate the degree of

equivalence between the submodel and the macroelement. In this case, it is proposed equivalence in terms of stored elastic strain energy. Below the variables intervening the method are defined.

Vector *{δ}* consists of the set of *h* master dofs. In this particular case it has 18 components, being the 3 linear displacements (*x*, *y* and *z*) of each of the 6 interface nodes, as explained before. Each vector $\{\delta\}_i$ defines a displacement case *i*, being *n* the total number of cases. Matrix *[δ]* consists of the *n* vectors *{δ}* in columns, which dimension is *h* x *n*.

$$\{\delta\}_i = \begin{Bmatrix} \delta_1 \\ \delta_2 \\ \cdots \\ \delta_h \end{Bmatrix} \tag{13}$$

The submodel elastic strain energy is called *U*. It is a scalar value solely dependent on displacements *{δ}*. Therefore, an energy value U_i is obtained per displacement case *i*. If the calculation for *n* cases is repeated, the result is a vector *{U}* of *n* components. This vector is calculated once only and it is invariable, since it defines the reference energy per displacement case. Information on the submodel is found in this vector.

$$U_i = U(\{\delta\}_i) \tag{14}$$

$$\{U\} = \{U_1 \quad U_2 \quad \cdots \quad U_n\} \tag{15}$$

Parameters are denominated A_j and the vector $\{A\}$ is that comprising the total number of parameters p of the problem. For this macroelement, value p equals 8. As mentioned already, the parameters are radii of each circular section beam element.

$$\{A\} = \begin{Bmatrix} A_1 \\ A_2 \\ \cdots \\ A_p \end{Bmatrix} \tag{16}$$

The macroelement elastic strain energy is called V. As in the case of U, it is also a scalar value and dependent not only on displacements $\{\delta\}$, but also parameter values. Vector column $\{V\}$ comprises the n components V_i.

$$V_i = V(\{\delta\}_i, \{A\}) \tag{17}$$

$$\{V\} = \{V_1 \quad V_2 \quad \cdots \quad V_n\} \tag{18}$$

3.1 Equation arrangement.

The aim of the method consists of calculating parameter value (16) to minimize the error between the submodel and macroelement elastic strain energies U and V. For both entities the equivalence must be satisfied for any $\{\delta\}_i$. Thus a non linear system of equations will be obtained equaling each U_i to the corresponding V_i, the later being a value depending on the parameters. Should the number of equations be equal to the number of parameters (n=p), then under normal conditions there would be solution

satisfying energy equality in each displacement case. In fact, the demand for a model representing a sufficiently wide range of displacement fields means the number of equations must be greater than the number of parameters (*n>>p*). This leads to a system without an exact solution, thus the choice adopted must determine the parameter values for the best possible equation adjustment. The most widely used method in these cases is that of Least Squares.

Resolution of the non-linear equation system will be performed iteratively. The function of the macroelement elastic strain energy will be linearized in each iteration via its first order Taylor series development:

$$V_i^{k+1} \approx V_i^k + \sum_{j=1}^{p} \frac{\partial V_i^k}{\partial A_j^k} \cdot (A_j^{k+1} - A_j^k) \tag{19}$$

k being the sub-index indicating the iteration number. Sub-index *i* corresponds to displacements case. To obtain this approximation there must be calculated first order partial derivatives. These derivatives are calculated using centered finite differences with the following formula:

$$\frac{\partial V_i}{\partial A_j} = \frac{V_i(A_1, A_2, \ldots A_j + \Delta A_j, \ldots A_p) - V_i(A_1, A_2, \ldots A_j - \Delta A_j, \ldots A_p)}{2 \cdot \Delta A_j} \tag{20}$$

where the value ΔA_j has been defined as $\Delta A_j = m A_j$. Value *m* is between 0 and 1. The fact of calculating these derivatives numerically is due to the complexity of the analytical form of the elastic strain energy function. Indeed, calculation of this function would imply obtaining the symbolic inversion of big matrices.

Applying Eq. (20) for each displacement and each parameter, the sensitivity matrix of dimensions *n* x *p* can be obtained.

$$\left[\frac{\partial V}{\partial A}\right]=\begin{bmatrix} \frac{\partial V_1}{\partial A_1} & \frac{\partial V_1}{\partial A_2} & \cdots & \frac{\partial V_1}{\partial A_p} \\ \frac{\partial V_2}{\partial A_1} & \frac{\partial V_2}{\partial A_2} & \cdots & \frac{\partial V_2}{\partial A_p} \\ \cdots & \cdots & \cdots & \cdots \\ \frac{\partial V_n}{\partial A_1} & \frac{\partial V_n}{\partial A_2} & \cdots & \frac{\partial V_n}{\partial A_p} \end{bmatrix} \tag{21}$$

Taking into account all the above, the following linearized equation system is formulated for *k* iteration, where approximate elastic strain energy is equaled to the submodel energy for each displacement case *i*.

$$\begin{aligned} &U_i = V_i^k + \sum_{j=1}^{p} \frac{\partial V_i^k}{\partial A_j^k} \cdot (A_j^{k+1} - A_j^k) \\ &i = 1, \ldots n \end{aligned} \tag{22}$$

This system must be solved for each iteration *k* via the Least Squares Method, for which the *R* error function is defined as follows:

$$R(\{A\}^{k+1}) = \sum_{i=1}^{n} \left(U_i - V_i^k - \sum_{j=1}^{p} \frac{\partial V_i^k}{\partial A_j^k} \cdot (A_j^{k+1} - A_j^k) \right)^2 \tag{23}$$

To obtain values which minimize the error function the derivatives must be equaled to zero for each parameter. Thus, the following determined compatible equation system is reached of *p* equations and *p* variables.

$$\frac{\partial R(\{A\}^{k+1})}{\partial A_j^{k+1}} = 0 \qquad j = 1, \ldots p \tag{24}$$

The solution of this system is the $\{A\}^{k+1}$ parameter vector. Set out below are the stop criteria taken into account in the iterative process.

3.2 Stop criteria.

To assess the degree of equivalence of the macroelement a value comparing the vectors *{U}* and *{V}* must be defined. The following formula is highly appropriate for this case:

$$\varepsilon = \sqrt{\frac{\sum_{i=1}^{n} \left(U_i - V_i^{k+1}\right)^2}{n}} \tag{25}$$

With Eq. (25) it can be evaluated the error committed in each iteration. In the general case, as this is a Least Squares method, it will not get a zero error. Therefore, the most interesting stop criterion is that which values stabilization of the error committed. When the error percentage increase in two consecutive iterations is less than a certain *q* value, the iterative process may be deemed finished.

$$\left|\frac{\varepsilon^{k+1}-\varepsilon^{k}}{\varepsilon^{k}}\right| < q \tag{26}$$

In Eq. (26) the absolute value is used because the error is expected to be less in each iteration if the method converges. As an additional criterion it can also be used the one based on the optimization parameters variation norm (27).

$$\left\|\{A\}^{k+1}-\{A\}^{k}\right\| = \sqrt{\sum_{j=1}^{p}\left(A_j^{k+1}-A_j^{k}\right)^2} < q' \tag{27}$$

However, it must be borne in mind, that it is highly likely there will be a certain number of parameters whose variation has no decisive impact on the objective function value. Therefore, prior to assessing the application of Eq. (27), a detailed study must be performed on parameter sensitivity, as explained in the parameter control section.

3.3 Initial approximation.

The selection of initial approximation tasks requires special care, since it has been verified the method used is highly sensitive to said choice, both in process duration and stability. Here the use of genetic algorithm techniques has been chosen. A simple genetic code in real numbers with 5 digits in decimal base indicating the value of optimization variables has been used for this. The variables chosen for the genetic algorithm will be detailed in the results section.

3.4 Parameter control.

Among the optimization methods, this one belong to those of steepest descend or gradient. The difference between the vector obtained as a solution and the previous in each iteration provides a direction vector of maximum gradient. This means that varying the parameters in this direction, a maximum variation of the objective function is achieved. This vector may be distorted in some cases. This is because the variation of some parameters has almost a null impact on the objective function; whereby its value may increase disproportionately without appreciable improvement in the solution. To prevent situations of this kind an increase control has been applied to the parameters. This control consists of applying a maximum value allowed. Once the maximum gradient vector has been obtained, variation of each parameter is calculated. If all values are lower than the percentage permitted, the process continues unchanged. Should said value be exceeded, the vector is scaled taking it to the allowed limit. This action prevents any parameter from growing exaggeratedly yet continues to maintain the maximum variation direction. The maximum variation value allowed is a parameter which may be either variable or fixed. Should it be variable, the most logical would be for it to decrease as the solution approaches optimum, to prevent leaping to another solution. In this study a fixed *f* value was chosen.

Apart from delimiting the parameter maximum percentage variation, sometimes a compromise decision must be taken in relation to the value of some of them. Applicable to the extreme cases commented above of parameters varying disproportionately, without hardly any improvement in the solution. This behavior may be quantified using the information provided by the sensitivity matrix. Each matrix term indicates the variation in elastic strain energy V_i for a unit value increase in the corresponding parameter. When this value is close to zero, it means the energy hardly varies. This

value may be very low for one displacement case and high for another. Therefore, a value which considers all cases must be taken as a reference. This value has been defined as S_j, for each parameter. It must be calculated in each iteration since the sensitivity matrix also varies.

$$S_j = \sqrt{\frac{\sum_{i=1}^{n}\left(\frac{\partial V_i}{\partial A_j}\right)^2}{n}} \tag{28}$$

The value obtained in Eq. (28) includes the objective function sensitivity for all displacement cases in relation to parameter A_j. As previously indicated, this sensitivity enables function invariance evaluation in relation to the parameter in question.

3.5 Flow diagram of the optimization process and term glossary.

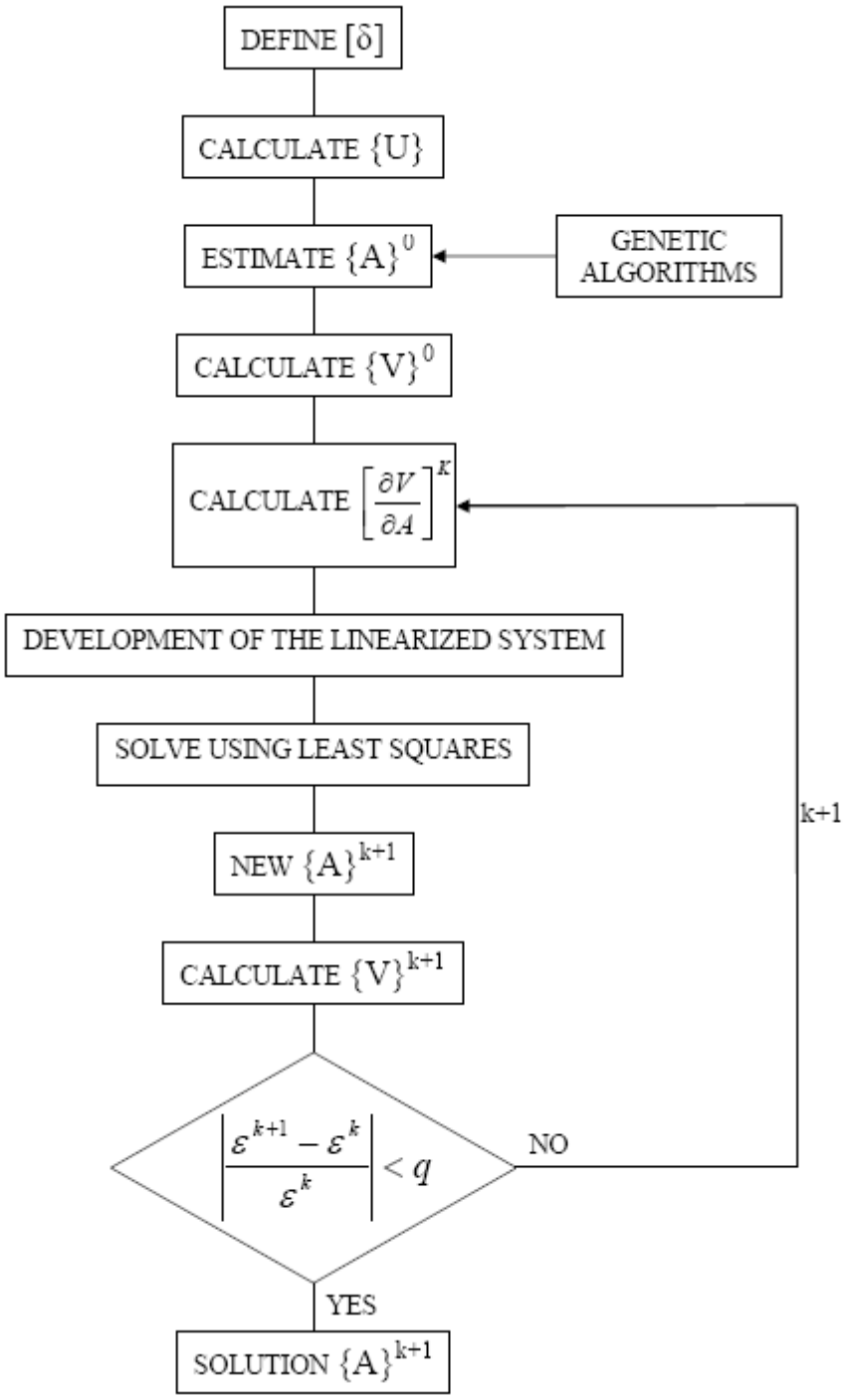

Fig. 8. Flow diagram of the optimization process

Term glossary.

n	total number of displacement cases
i	subindex of current displacement case
h	number of displacement vector dofs
$\{\delta\}_i$	displacement vector of case i
$[\delta]$	vector displacement matrix
U_i	elastic strain energy of the model for case i
$\{U\}$	vector of elastic strain energies of the model
V_i	macroelement elastic strain energy for case i
$\{V\}$	vector of macroelement elastic strain energies
p	total number of parameters
j	current parameter subindex
A_j	parameter j
$\{A\}$	parameter vector
m	increasing percentage of parameters in numerical derivation
$\left[\frac{\partial V}{\partial A}\right]$	sensitivity matrix
k	iteration number
R	error or objective function
ε	absolute error
q	relative error
f	maximum variation in parameters control
S_j	parameter j sensitivity

4. Results.

This section sets out the optimization process results applied to the macroelement described in section 2. The material used is aluminum with the following characteristics:

Young module:	E = 70 GPa
Shear module:	G = 27 GPa
Poisson Coefficient:	υ = 0.33

Method application conditions:

Number of macroelement parameters:	p = 8
Number of master dofs:	h = 18
Number of displacement cases:	n = 60
Increased percentage in the sensitivity matrix calculation:	m = 0.01
Maximum Number of iterations:	k_max = 15
Value of admissible q:	q = 0.5 %
Maximum variation in parameter control:	f = 10 %

Step one is to create the 60 displacement cases, for which vectors $\{\delta\}$ are created randomly. The magnitudes of these displacements were chosen so they were higher than expected for the usual working conditions of the real joint. Thus, it is guaranteed correct macroelement behavior under normal conditions. The random function (29) is centered at zero with values between -10^{-5} and 10^{-5} meters.

$$\delta = 10^{-5} \cdot (2 \cdot Random - 1) \tag{29}$$

Once created the matrix *[δ]* with the 60 vectors *{δ}* each of 18 components, vector *{U}* is calculated. This vector can be obtained in different ways, the most common being calculation of the model elastic strain energy for each displacement case as per the following formula:

$$U_i = \frac{1}{2} \cdot \{\delta\}_i^T \cdot \{F\}_i \tag{30}$$

{F} being the vector comprising components of reaction forces associated to master dofs where displacements are applied. Repeating Eq. (30) for all displacement cases, the vector *{U}* is obtained. As mentioned previously this vector is only calculated once.

The search for initial approximation $\{A\}^0$ was carried out executing the free Genetic Algorithm code "Pikaia" [19]. The values adopted for the algorithm values are as follows:

Number of individuals in the population:	150
Number of generations in the evolution:	400
Encoding:	decimal
Number of digits to encode e genotype:	5
Crossover probability:	0.85
Mutation mode: adjustable rate based on fitness	
Initial mutation rate:	0.005

Minimum mutation rate:	0.0005
Maximum mutation rate:	0.25
Reproduction plan: full generational replacement	
Elitism:	active

In this work it was decided to limit the parameter value bearing in mind the physical features of the submodel. On the other hand, the search space was notably reduced taking into account the symmetry extant in the submodel, which implies a certain relationship “a priori” among some parameters.

After 400 generations the values obtained for initial approximation (expressed in millimeters) were the following:

$$\{A\}^0 = [8.989 \quad 8.999 \quad 25.000 \quad 25.000 \quad 10.917 \quad 10.822 \quad 4.971 \quad 2.810]^T$$

These are the values initially defining the macroelement; i.e. the values of the 8 radii of the circular section beams forming the same. Now the elastic strain energy V_i can be calculated for each displacement case. By calculating these values for the 60 cases, vector *{V}* is formed. Now, it can be assessed the degree of equivalence between the macroelement and the submodel, using the Eq. (25), which obtained a value of ε = 0.0292.

Fig. 9 represents the quadratic difference values of the *U* and *V* energies per displacement case *i*. This figure confirms the *V* values are considerably similar to those of *U*.

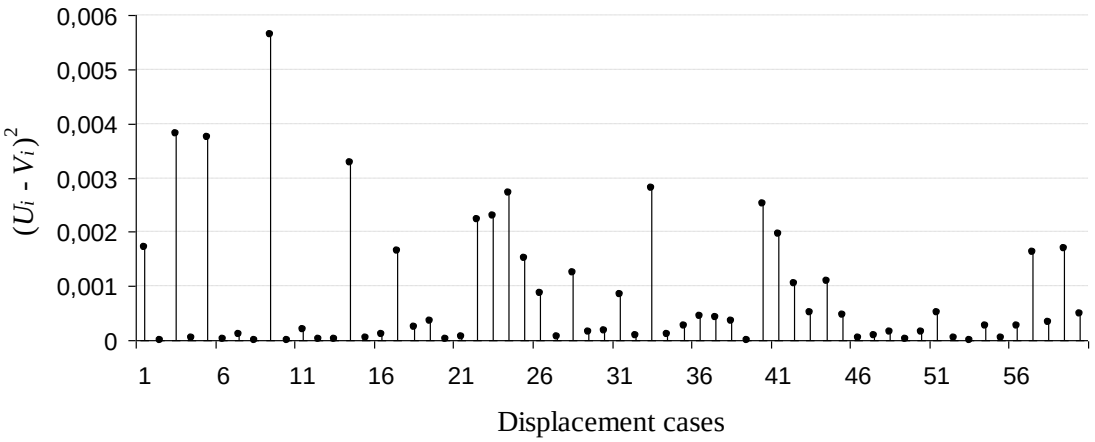

Fig. 9. Difference between U and V energies for the 60 displacement cases.

Taking this initial approximation, the method described in the previous section is applied to refine the parameter values. Fig. 10 shows the evolution of the error (ε) after 10 iterations. It can be seen how it diminishes in each iteration, although each time with less intensity. Complete equivalence is impossible to achieve, since the macroelement has considerably fewer elements than the submodel. The macroelement purpose is to approximately represent the mechanical behavior of the submodel. In iteration k=10 the iterative process stop requirement is met: relative error q is now under 0.5 %.

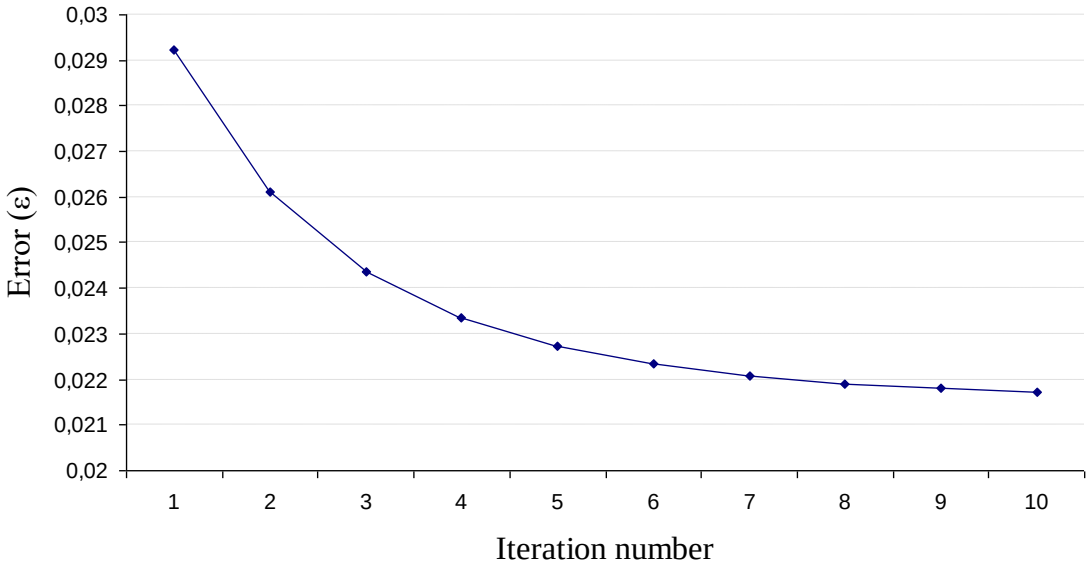

Fig. 10. Error evolution.

In these 10 iterations the error has reduced from 0.0292 to 0.0217, i.e. equal to a reduction of 25.64 %. Therefore, application of the method has considerably improved the initial solution. However, prior to considering the results correct, parameter variation needs to be studied in greater detail.

Fig. 11 shows the parameter evolution in each iteration. Table 1 shows numerical values for the parameters in iterations one and ten, likewise their increase as a percentage. Growth of parameter 4 stands out because it goes beyond the limits. This parameter has an anomalous behavior as mentioned in the previous section. It grows disproportionately although error reduction is hardly significant.

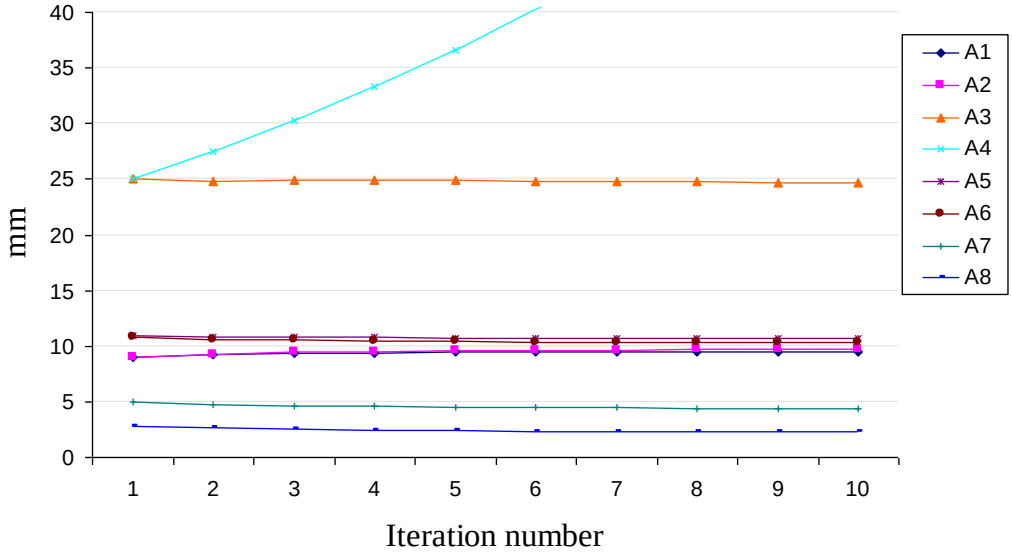

Fig. 11. Parameter evolution.

Table 1. Values of parameters and their relative variation.

	A1	A2	A3	A4	A5	A6	A7	A8
Iter. 1	8,989	8,999	25,000	25,000	10,917	10,822	4,971	2,810
Iter. 10	9,510	9,691	24,687	58,949	10,704	10,346	4,417	2,290
%	5,798	7,696	-1,250	135,795	-1,958	-4,397	-11,145	-18,511

Fig. 12 shows the parameter variation percentages. It can be seen all parameters except 4 have stabilized and reached their optimum value. This figure shows how parameters control acts, limiting the maximum increase *f* of any parameter at 10 % in each iteration.

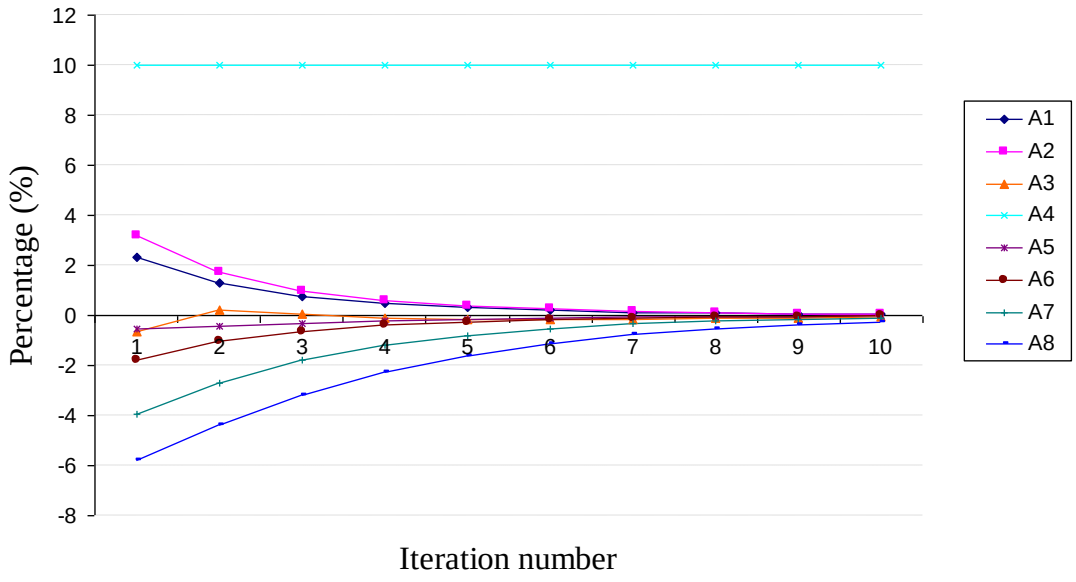

Fig. 12. Variation percentages of parameters.

The anomalous behavior of parameter 4 can be quantified using the information provided by parameter sensitivity S_j. The following table shows the values of S_j in each iteration.

Table 2. Parameter sensitivity values.

Iteration	S1	S2	S3	S4	S5	S6	S7	S8
1	11,91	10,36	0,45	0,86	12,92	14,97	6,64	3,99
2	12,41	10,75	0,53	0,56	12,88	15,63	6,54	3,80
3	12,73	10,99	0,57	0,36	12,95	16,04	6,46	3,66
4	12,93	11,15	0,60	0,23	13,03	16,31	6,41	3,56
5	13,06	11,25	0,62	0,15	13,10	16,49	6,37	3,49
6	13,15	11,31	0,64	0,09	13,15	16,61	6,34	3,44
7	13,20	11,35	0,66	0,06	13,19	16,69	6,32	3,41
8	13,24	11,38	0,67	0,04	13,22	16,74	6,31	3,38
9	13,26	11,40	0,67	0,02	13,24	16,78	6,30	3,37
10	13,27	11,41	0,67	0,01	13,25	16,81	6,30	3,37

It can be seen value S_4 is not only very low but diminishes on each iteration. This means the error hardly varies according to this parameter. Having got this far, a compromise decision must be taken which provides a solution with a low error and realistic parameter values. Paying attention to the submodel, it can be seen it has quite a high degree of symmetry. Results obtained via the energy equivalence method are very coherent with this fact. It is sufficient to observe the clear similitude among some parameter values. E.g. it can be compared the symmetry extant between parameters 1 and 2, likewise between 5 and 6. Furthermore, the values of both couples are quite similar. Macroelement parameters 3 and 4 would correspond to the central part of the joint on the submodel. Therefore it is logical to think they have very similar values, since in the submodel, this central part has a constant diameter. Therefore, a good solution would be to equal value A_4 to A_3. With this change, the error increases slightly to a value of 0.0237. Even so this error is 18.84 % less than that obtained with initial approximation. The results obtained with this method for the equivalence between the macroelement and the submodel are satisfactory, always within the limitations involved in drastically reducing the number of dofs of a system.

The number of displacement cases in the resolution of this specific case was set at n=60. With a view to fully demonstrating the macroelement validity obtained, 10 displacement groups were chosen. Group 1 was used to resolve this example and the other 9 groups created randomly, and the error calculated for each. Fig. 13 shows these values. The mean value is 0.0236, with a maximum deviation of 10%. With these data the value of n=60 is considered sufficient and the macroelement obtained valid for any displacement combination.

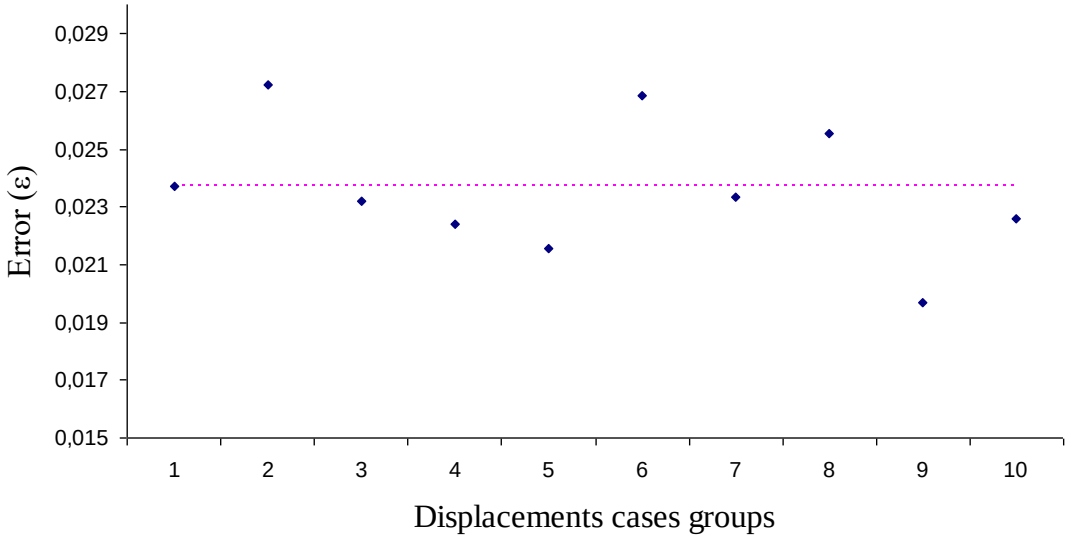

Fig. 13. Error comparison for several "displacement case groups".

5. Conclusions

The study purpose is centered on replacing the Finite Element model of an articulated VGT joint (with an elevated number of 3D elements including contact elements) with an equivalent parametric macroelement (EPM) with few elements. Therefore, a method was defined to minimize an objective function based on the equivalence of elastic strain energy absorbed by the two models. Thus, the aim is to find EPM parameter values which minimized this function.

The optimization method is based on the resolution of a non-linear redundant equation system, tackled via the Nonlinear Least Squares Method. For this an iterative diagram was proposed where the equations are linearized via the first order Taylor series development and subsequently solved via a Least Squares Method. This optimization is based on an initial solution via genetic algorithms.

The equivalence degree achieved for the EPM has been satisfactory. The adjustment percentage for different load cases over the reduced VGT exceeded 99 % in relation to the original detailed model while the analysis time has decreased in two orders of magnitude.

Acknowledgements

The authors wish to acknowledge the financial support received from the Ministry of Education and Science of Spain, through the subsidy of research project DPI2005-05417.

References

[1] Miura K., Furuya H. and Gokhale D. Variable Geometry truss and its application to deployable truss and space crane arm. Acta Astronautica 1985;12;7:599-607.

[2] Gun-shing Chen and Wada B. K. Adaptive Truss Manipulator Space Crane Concept. Journal of Spacecraft and Rocket 1993;30;1:11-5.

[3] Stoughton R. S., Tucker J.C., Horner C.G. A Variable Geometry Truss Manipulator For Positioning Large Payloads. In: American Nuclear Society Topical on Robotics and Remote Handling Conference, Monterey, California, USA. 1995:1-8.

[4] Hughes P. C. ; Sincarsin W. G. ; Carroll K. A. Trussarm-A variable Geometry Truss Manipulator. Journal of intelligent material systems and structures. 1991;2;2:148-60.

[5] Sircasin W. G. and Hughes P. C. Trussarm Candidate Geometries, Dynacon Report 28-611/0401. 1987.

[6] Arun V., Reinholtz C. F. and Watson L. T. Enumeration And Analysis Of Variable Geometry Truss Manipulators. Proceedings of ASME Mechanisms Conference 1990:93-8.

[7] Shengyang Huang, Natori M.C. and Miura K. Motion Control of Free-Floating Variable Geometry Truss. Part 1: Kinematics. Journal of Guidance, Control and Dynamics 1996;4;19:756-63.

[8] Williams II R.L. and Hexter IV E.R. Maximizing Kinematic Motion For A 3-Dof VGT Module. Journal of Mechanical Design 1998;120;2:333-36.

[9] Chen Wu-Jun, Luo Yao-Zhi, Fu Gong-Yi, Gong Jing-Hai and Dong Shi-Lin. A Study on Space Masts Based on Octahedral Truss Family. International Journal of Space Structures 2001;1;16:75-82.

[10] Guyan J. Reduction of Stiffness and Mass Matrices. AIAA 1965;3:380.

[11] Wilson Edward L. The static condensation algorithm. Journal for numerical methods in engineering 1974;8:198-203.

[12] Friswell M. I. Model Reduction Using Dynamic and Iterated IRS Techniques. Journal of Sound and Vibration 1995;186:311-23.

[13] Friswell M. I. The Convergence Of The Iterated IRS Method. Journal of Sound and Vibration 1998;211:123-32.

[14] Parsons Thomas J., GangaRao Hota V. S. and Peterson William C. Macro-element Analysis. Computer and Structures 1985;20:877-83.

[15] Kwan A. S. K. and Pellegrino S. Matrix Formulation of Macro-elements for Deployable Structures. Computer and Structures 1994;50:237-54.

[16] Carpenter Donald L. and Snyder Virgil W. Implementation of Substructuring in Finite Elements. Proceedings of the Third Engineering Mechanics Division Specialty Conference, Austin, Texas 1979:377-79.

[17] Fernández-Bustos, I. , Aguirrebeitia, J., Avilés, R. Angulo, C. Kinematical Synthesis of 1-dof Mechanisms Using Finite Elements and Genetic Algorithms, Finite Elements in Analysis and Design 2005;41;15:1441-63.

[18] Avilés, R , Ajuria, G., Amezua, E., Gómez-Garay, V. Finite Element Approach to the Position Problems in Open-loop Variable Geometry Trusses. Finite Elements in Analysis and Design 2000;34;3-4:233-55.

[19] Charbonneau, P. An Introduction to Genetic Algorithms for Numerical Optimization. NCAR Technical Note 450+IA (Boulder: National Center for Atmospheric Research);2002.

Appendix. Element stiffness matrices.

$$\begin{bmatrix}
\frac{E\cdot A}{L} & 0 & 0 & 0 & 0 & 0 & -\frac{E\cdot A}{L} & 0 & 0 & 0 & 0 & 0 \\
0 & \frac{12\cdot E\cdot I_z}{L^3} & 0 & 0 & 0 & \frac{6\cdot E\cdot I_z}{L^2} & 0 & -\frac{12\cdot E\cdot I_z}{L^3} & 0 & 0 & 0 & \frac{6\cdot E\cdot I_z}{L^2} \\
0 & 0 & \frac{12\cdot E\cdot I_y}{L^3} & 0 & -\frac{6\cdot E\cdot I_y}{L^2} & 0 & 0 & 0 & -\frac{12\cdot E\cdot I_y}{L^3} & 0 & -\frac{6\cdot E\cdot I_y}{L^2} & 0 \\
0 & 0 & 0 & \frac{G\cdot J}{L} & 0 & 0 & 0 & 0 & 0 & -\frac{G\cdot J}{L} & 0 & 0 \\
0 & 0 & -\frac{6\cdot E\cdot I_y}{L^2} & 0 & \frac{4\cdot E\cdot I_y}{L} & 0 & 0 & 0 & \frac{6\cdot E\cdot I_y}{L^2} & 0 & \frac{2\cdot E\cdot I_y}{L} & 0 \\
0 & \frac{6\cdot E\cdot I_z}{L^2} & 0 & 0 & 0 & \frac{4\cdot E\cdot I_z}{L} & 0 & -\frac{6\cdot E\cdot I_z}{L^2} & 0 & 0 & 0 & \frac{2\cdot E\cdot I_z}{L} \\
-\frac{E\cdot A}{L} & 0 & 0 & 0 & 0 & 0 & \frac{E\cdot A}{L} & 0 & 0 & 0 & 0 & 0 \\
0 & -\frac{12\cdot E\cdot I_z}{L^3} & 0 & 0 & 0 & -\frac{6\cdot E\cdot I_z}{L^2} & 0 & \frac{12\cdot E\cdot I_z}{L^3} & 0 & 0 & 0 & -\frac{6\cdot E\cdot I_z}{L^2} \\
0 & 0 & -\frac{12\cdot E\cdot I_y}{L^3} & 0 & \frac{6\cdot E\cdot I_y}{L^2} & 0 & 0 & 0 & \frac{12\cdot E\cdot I_y}{L^3} & 0 & \frac{6\cdot E\cdot I_y}{L^2} & 0 \\
0 & 0 & 0 & -\frac{G\cdot J}{L} & 0 & 0 & 0 & 0 & 0 & \frac{G\cdot J}{L} & 0 & 0 \\
0 & 0 & -\frac{6\cdot E\cdot I_y}{L^2} & 0 & \frac{2\cdot E\cdot I_y}{L} & 0 & 0 & 0 & \frac{6\cdot E\cdot I_y}{L^2} & 0 & \frac{4\cdot E\cdot I_y}{L} & 0 \\
0 & \frac{6\cdot E\cdot I_z}{L^2} & 0 & 0 & 0 & \frac{2\cdot E\cdot I_z}{L} & 0 & -\frac{6\cdot E\cdot I_z}{L^2} & 0 & 0 & 0 & \frac{4\cdot E\cdot I_z}{L}
\end{bmatrix}$$

Fig. 14. Stiffness matrix of elements 1,2,3,4,5 and 6 in local coordinates

$$\begin{bmatrix}
\frac{E\cdot A}{L} & 0 & 0 & 0 & 0 & 0 & -\frac{E\cdot A}{L} & 0 & 0 & 0 & 0 & 0 \\
0 & \frac{3\cdot E\cdot I_z}{L^3} & 0 & 0 & 0 & 0 & 0 & -\frac{3\cdot E\cdot I_z}{L^3} & 0 & 0 & 0 & \frac{3\cdot E\cdot I_z}{L^2} \\
0 & 0 & \frac{12\cdot E\cdot I_y}{L^3} & 0 & -\frac{6\cdot E\cdot I_y}{L^2} & 0 & 0 & 0 & -\frac{12\cdot E\cdot I_y}{L^3} & 0 & -\frac{6\cdot E\cdot I_y}{L^2} & 0 \\
0 & 0 & 0 & \frac{G\cdot J}{L} & 0 & 0 & 0 & 0 & 0 & -\frac{G\cdot J}{L} & 0 & 0 \\
0 & 0 & -\frac{6\cdot E\cdot I_y}{L^2} & 0 & \frac{4\cdot E\cdot I_y}{L} & 0 & 0 & 0 & \frac{6\cdot E\cdot I_y}{L^2} & 0 & \frac{2\cdot E\cdot I_y}{L} & 0 \\
0 & 0 & 0 & 0 & 0 & 0 & 0 & 0 & 0 & 0 & 0 & 0 \\
-\frac{E\cdot A}{L} & 0 & 0 & 0 & 0 & 0 & \frac{E\cdot A}{L} & 0 & 0 & 0 & 0 & 0 \\
0 & -\frac{3\cdot E\cdot I_z}{L^3} & 0 & 0 & 0 & 0 & 0 & \frac{3\cdot E\cdot I_z}{L^3} & 0 & 0 & 0 & -\frac{3\cdot E\cdot I_z}{L^2} \\
0 & 0 & -\frac{12\cdot E\cdot I_y}{L^3} & 0 & \frac{6\cdot E\cdot I_y}{L^2} & 0 & 0 & 0 & \frac{12\cdot E\cdot I_y}{L^3} & 0 & \frac{6\cdot E\cdot I_y}{L^2} & 0 \\
0 & 0 & 0 & -\frac{G\cdot J}{L} & 0 & 0 & 0 & 0 & 0 & \frac{G\cdot J}{L} & 0 & 0 \\
0 & 0 & -\frac{6\cdot E\cdot I_y}{L^2} & 0 & \frac{2\cdot E\cdot I_y}{L} & 0 & 0 & 0 & \frac{6\cdot E\cdot I_y}{L^2} & 0 & \frac{4\cdot E\cdot I_y}{L} & 0 \\
0 & \frac{3\cdot E\cdot I_z}{L^2} & 0 & 0 & 0 & 0 & 0 & -\frac{3\cdot E\cdot I_z}{L^2} & 0 & 0 & 0 & \frac{3\cdot E\cdot I_z}{L}
\end{bmatrix}$$

Fig 15. Stiffness matrix of elements 7 and 8 in local coordinates

The row and column corresponding to the released dof θ_{z1} all contain zeros. In this component, these elements do not contribute stiffness to the macroelement.

Figure Legends:

Tables: